

Lasers in Manufacturing Conference 2023

# Distribution of SFTC, NbC, and Cr<sub>3</sub>C<sub>2</sub> particles in Aluminium Bronze by laser melt injection

Minkeshkumar Ramoliya<sup>a,\*</sup>, Annika Bohlen<sup>a</sup>, Thomas Seefeld<sup>a, b</sup>

<sup>a</sup>BIAS – Bremer Institut fuer angewandte Strahltechnik GmbH, Klagenfurterstrasse 5, 28359 Bremen, Germany

<sup>b</sup>MAPEX Center for Materials and Processes – University of Bremen, Bibliothekstrasse 1, 28359 Bremen, Germany

---

## Abstract

Ship propellers made of copper-based alloys are subject to high wear due to cavitation, which reduces service life. Metal matrix composite (MMC) layers have demonstrated considerable potential for enhancing wear resistance. Laser melt injection (LMI) is used to generate MMC layers on the aluminium bronze substrate by injecting spherical fused tungsten carbide, niobium carbide, and chromium carbide. In particular, the influences of the processing parameters, laser power, and powder flow rate on the microstructure of the MMC layers have been examined. Typical dimensions of single tracks are a width of 4 mm and a depth of 1 mm. The particle content in the MMC layers is determined by assessment of the metallographic cross-section of micrographs and is about 25% - 45%. An important finding is that a homogenous particle distribution can be achieved across the entire depth and width of the melt pool.

Keywords: laser melt injection; MMC; cavitation erosion; homogenous particle distribution

---

## 1. Introduction

The copper-based aluminium bronze (AlBz) alloys are extensively used in shipbuilding, due to their excellent mechanical properties such as high strength-to-weight ratio, superior corrosion resistance, and good creep fatigue and toughness properties. High friction and weak wear resistance of the material preclude its usage in a number of applications. The ease of casting and welding are these alloys' key advantages. Ship propellers, valve components, couplings, and pumps often make up most items produced with this family of alloys. Additionally, the potential for restrengthening after service problems can save production and maintenance

---

\* Corresponding author. Tel.: +49-421-218-58068; fax: +49-421-218-58063.  
E-mail address: ramoliya@bias.de.

expenses. Although these alloys have good qualities, the service circumstances in seawater and under alternating loads necessitate controlling their corrosion behavior and improving wear performances. The surface is typically where the component breakdown processes begin. AlBz alloys are susceptible to environmentally assisted cracking (EAC), which increases failure size over time, claim Koul et al. Cavitation erosion is one of the most common AlBz propeller failure types in marine environments, and it is significantly impacted by the material's surface properties. Additionally, fatigue phenomena will be brought on by the cyclic loads placed on the propeller blades while they are in operation in the corrosive environment of seawater. It should be noted that surface defects in the material are where fatigue cracks often start to form. As a result, marine alloy surfaces must be reinforced (Mousavi et al. 2021).

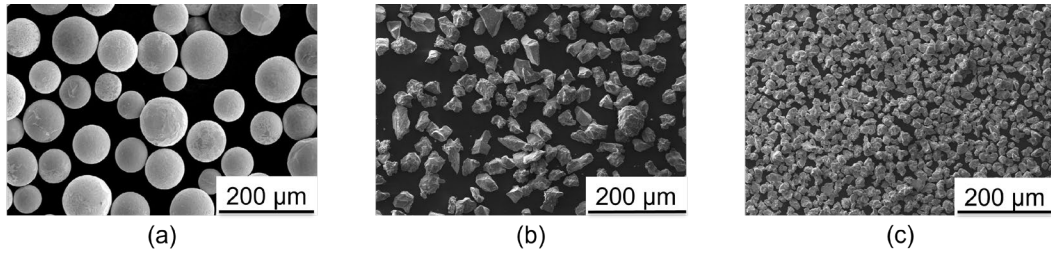
In contrast, their prospective applications are limited by their high friction coefficient and poor wear resistance, particularly to fields requiring precise surface capabilities. The addition of a surface MMC layer is one potential method for improving the surface properties of copper-based alloys without altering their bulk properties. Laser melt injection (LMI) is believed to be the best method for creating MMC layers on nickel-aluminium bronze alloys. The top layer of the metal substrate is melted using a laser beam during the LMI process, and the melt pool is simultaneously loaded with an additive powder. Particles are caught during the melt pool's quick solidification, and an MMC layer develops. The interaction of the injected particles with the melt is minimal because the laser beam's contact with the particles is constrained. The abrupt contact between the coating and the substrate that is typically seen in laser cladding is also eliminated by injecting the ceramic particles directly into the melt pool of the substrate (Chen et. al. 2008). Due to their high degree of hardness, resistance to abrasion, corrosion, and compatibility with metal matrix, carbides rank among the best ceramic reinforcements for metal matrix in MMCs. For MMCs, the most common types of carbide reinforcement particles that have been used to date are tungsten carbide (WC), titanium carbide (TiC), niobium carbide (NbC), and vanadium carbide (VCp) (Li et. al. 2021). For instance, an MMC surface made of Cu-based aluminium bronze supplemented with spherical fused tungsten carbide particles can significantly increase wear resistance. The matrix material can be reinforced to reduce abrasive wear to 25% (Freiße et. al. 2021). However, there is a lack of studies on the laser production of surface NbC and Cr<sub>3</sub>C<sub>2</sub> reinforced MMCs on AlBz alloy for enhancing wear and corrosion resistance.

The ability to withstand abrasive wear improves with hard particle composition. A non-homogenous particle distribution may occasionally result from the LMI parameters. This could be detrimental if the LMI process is intended to produce a finished surface with a high hard particle content. As a result, this work examines the particle distribution for MMCs made of aluminium bronze reinforced with spherical fused tungsten carbide, niobium carbide, and chromium carbide.

## **2. Experimental**

### *2.1. Materials*

Spherical fused tungsten carbide, chromium carbide, and niobium carbide were used as reinforcing particles. The SEM images of these reinforcing particles have been shown in Fig. 1. Their corresponding densities were 15.63 g/cm<sup>3</sup>, 6.68 g/cm<sup>3</sup>, and 7.82 g/cm<sup>3</sup>, respectively. Aluminium bronze (CuAl10Ni5Fe4) was employed as the matrix material with dimensions of 50 mm length, 20 mm width, and 12 mm height. The used aluminium bronze has a density of 7.6 g/cm<sup>3</sup> and is a typical alloy for marine applications such as propellers.



Ramoliya 2023

BIAS ID 230181

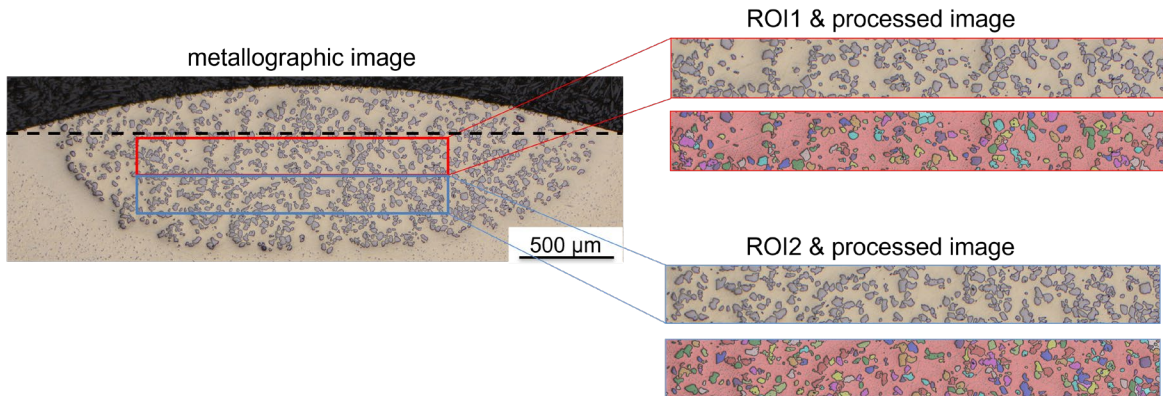
Fig. 1. SEM images of reinforcements particles (a) spherical fused tungsten carbide, (b) chromium carbide, and (c) niobium carbide.

## 2.2. Set-up

A Trumpf TruDisk 12002 Yb:YAG disk laser with a maximum output power of 12 kW had been used for the LMI process. A 200  $\mu\text{m}$ -diameter laser light wire directs the beam to the processing equipment. A 3-axis CNC is being used as the traversing unit. The discrete coaxial GTV PN6625 six-jet nozzle with a working distance of 25 mm received the carbide powder from an Oerlikon Metco Twin 150 rotating disk powder feeder. A volume flow rate of the powder feeding gas between 2 l/min and 7 l/min is used.

## 2.3. Procedure

An MMC layer was created with varying laser power and powder feed rates while maintaining a constant process velocity. The laser spot diameter throughout the experiment has been set at 3 mm, while the defocusing distance is 21 mm.



Ramoliya 2023

BIAS ID 230178

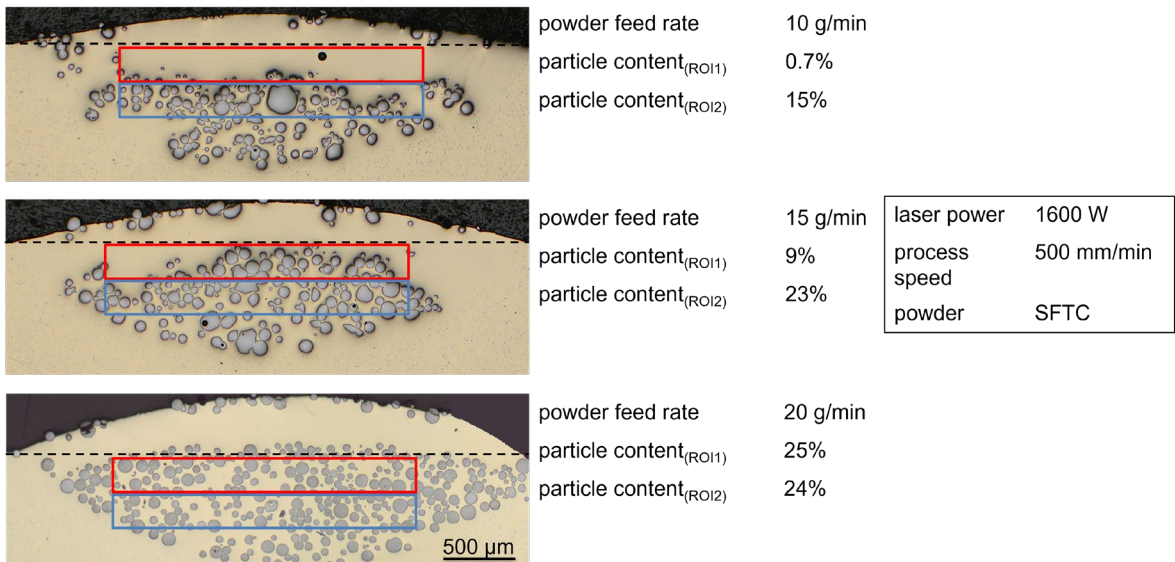
Fig. 2. Cross-section of an MMC layer with ROIs for evaluating the particle distribution.

The prepared MMC specimens were thus cut using EDM, and the cross sections were polished and ground. For each reinforced layer, different areas of interest (ROIs) were designated along the cross-section (see Fig. 2). The ROIs' hard particle distribution was examined using automated image processing, which filtered and binarized the image. Comparative analysis was done on the hard particle distribution within two ROIs for

each reinforced layer. This reveals the layer's homogeneity. The specimen's initial surface (dashed line) is where the tops of the ROIs meet because this is where the particle distribution is most intriguing.

### 3. Results and discussions

A single-track MMC layer based on various laser powers and powder feed rates was used to study the effects of factors on the distribution of hard particles. Spherical fused tungsten carbide particles with particle sizes ranging from 45 to 110  $\mu\text{m}$  are employed as reinforced particles. The volume fraction of SFTC inside the track lies in the range of up to 25%. SFTC provides a crack-free MMC layer. The processing window for the SFTC particles with a constant feed rate of 500 mm/min can be achieved with laser power between 1500 – 1800 W, and a powder flow rate between 10 – 20 g/min. The length of a single laser track is about 40 mm, the width is about 4 mm, and the maximum depth is about 1 mm. The particle-free zone can be found above all MMC levels. The examples are shown in Fig. 3. The spherical fused tungsten carbide particles (15.63 g/cm<sup>3</sup>) have a larger density than the aluminium bronze matrix (7.6 g/cm<sup>3</sup>), which is the cause of this deposition. This phenomenon can be reduced by lowering the process velocity and increasing the powder feed rate. Pei claims that the solidification of the melt pool displays how process velocity influences particle distribution. The viscosity of the melt pool enhances throughout solidification until the melt pool is entirely solidified. Because of the increased viscosity, particles that join the melt pool later in the process pierce it less deeply, leading to grading (Pei et al., 2002). The difference in the particle content of both ROIs of MMC layers produced with 10g/min, 15 g/min, and 20 g/min powder feed rates is 14.3%, 14%, and 1% respectively (see Fig. 3). The SFTC particles with 20 g/min powder feed rates are therefore said to be equally distributed underneath the initial surface.



Ramoliya 2023

BIAS ID 230180

Fig. 3. Micrograph of the laser melt injected surface cross-section with spherical fused tungsten carbides with ROIs.

To find the best set of laser processing parameters for chromium carbide, cross-sections of single laser tracks made with various laser and powder parameters are evaluated. The diameter of the chromium carbide

was in the range of 45 – 106  $\mu\text{m}$ . The width of a single laser track is about 3 mm, and the maximum depth is about 0.7 mm. From Fig. 4, the particles were found on the upper part of the layer. The reason for that could be the lower density of chromium carbide particles. The laser power directly influences the distribution of  $\text{Cr}_3\text{C}_2$  particles in the bead cross-section and their volume percentage. The reinforced particles in the alloy matrix were completely dissolved because of the lower melting point of chromium carbide as the laser power was increased further. In addition to ensuring a more equal distribution of particles in the bead cross-section, the increased laser power also causes more intense fluid flow in the molten pool, simultaneously raising particle dissolution. Additionally, pores are detected in the layer. Pores were also visible in the melted particle (see Fig. 4 (e)). The specimen showed an undesired melting or fusing of the particles. As depicted in Fig. 4 (d-f), the unwanted melting of the particles also rose when the laser's power remained constant while the flow rate of powder increased. It has been found that the optimal range of processing parameters is very narrow. The lower heat input generates the porous structure leading to high porosity while higher heat input dissolves more particles and their non-uniform distribution.

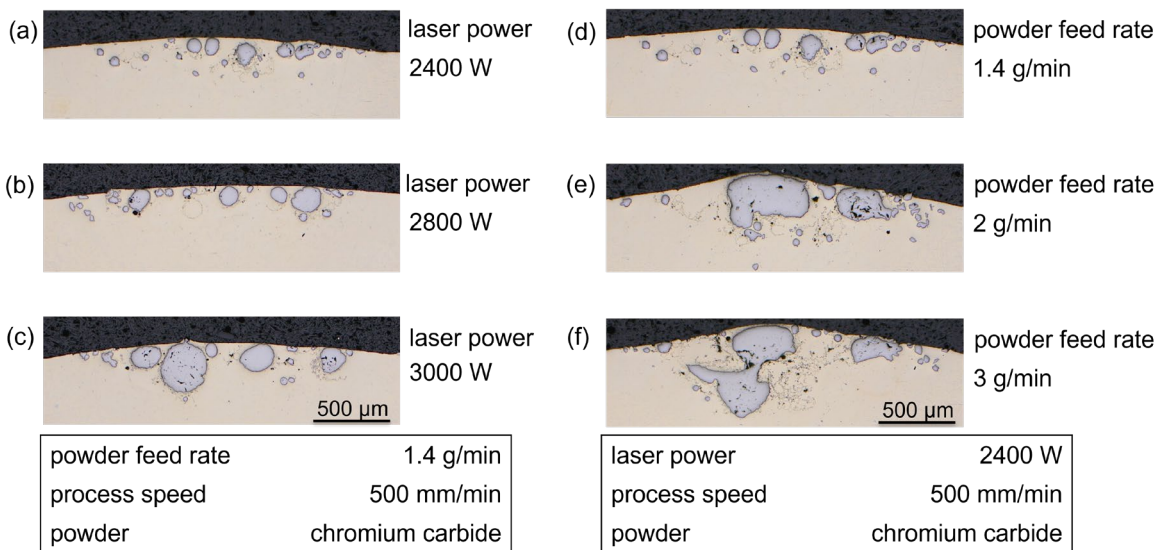


Fig. 4. Cross sections of an MMC layer made of chromium carbide, a-c) effect of laser power, and d-f) effect of powder feed rate.

The micrograph of the cross-section for the NbC-reinforced MMC layer is shown in Fig. 5. The diameter of the used powder particles was 10 – 63  $\mu\text{m}$ . To establish the range of optimal LMI parameters, a series of single-pass clad has been made at laser powers of 2000 W - 3000 W with traverse speeds of 500 mm/min. The powder feed rate was in the range of 3.0 to 5.0 g/min. The length of a single laser track is about 40 mm, the width is about 4 mm, and the maximum depth is about 1 mm. The suitable parameters were demonstrated to produce a single-pass clad with a uniform distribution of RPs throughout the matrix with no dissolution of particles. The parameter of a single track is  $P = 2800 \text{ W}$ ,  $v = 500 \text{ mm/min}$ , and  $m = 5 \text{ g/min}$ . NbC provides a crack-free MMC layer up to a particle content of 40%. It's important to consider that the particles are evenly distributed over the melt pool's entire depth and width. It is also proven by comparing the particle content in both ROIs. The particle contents of both ROIs were almost the same with a value of 16%. Hence, it can be said that the niobium carbide particles are homogeneously distributed. Niobium carbide can be distributed homogeneously at

greater laser powers and lower powder feed rates than SFTC can. That's because NbC's density is only roughly half that of SFTC. This suggests that the usage of NbC is economically advantageous because it only requires half the mass of SFTC to produce a given component.

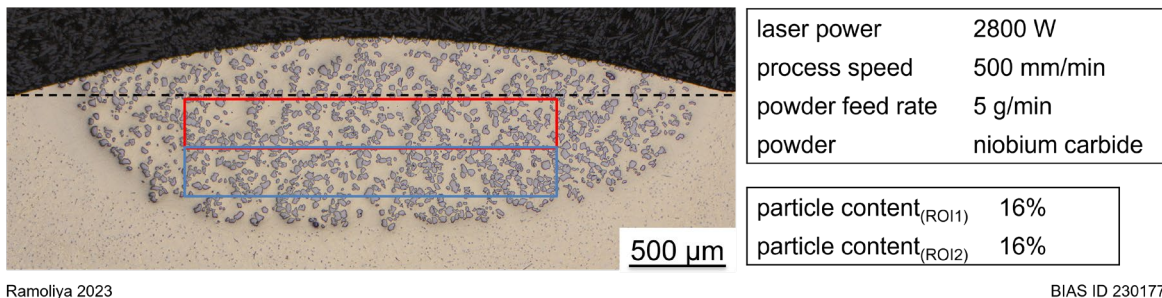


Fig. 5. Metallographic image of laser melt injected track of niobium carbide powder with ROIs.

#### 4. Conclusion

An Aluminium bronze-based MMC layer reinforced by SFTC, NbC, and  $\text{Cr}_3\text{C}_2$  particles has been produced using a laser melt injection process. This work investigated the distribution of the particles in the LMI of single tracks. A fine and homogenous distribution of niobium carbide and SFTC particles within the melt pool free of voids or other defects is possible while an MMC layer consisting of the chromium carbide particles showed pores and undesirable melting of the particles.

#### Acknowledgements

The ZIM-project no. KK5274702AG1 was funded by the Federal Ministry for Economic Affairs and Energy (BMWi) via the German Federation of Industrial Research Associations (AiF) in accordance with the policy to support the Central Innovations of Medium-Sized Enterprises (ZIM) based on a decision by the German Bundestag.



#### References

- Chen, Yanbin; Liu, Dejian; Li, Fuquan; Li, Liqun (2008): WCp/Ti-6Al-4V graded metal matrix composites layer produced by laser melt injection. In *Surface and Coatings Technology* 202 (19), pp. 4780–4787. DOI: 10.1016/j.surfcoat.2008.04.057.
- Freiße, H.; Langebeck, A.; Koehler, H.; Seefeld, T. (2016): Dry strip drawing test on tool surfaces reinforced by hard particles. *Dry Met. Forming OAJ FMT 2*, 001-006.
- Koul, M., & Gaies, J. (2013). An Environmentally Assisted Cracking Evaluation of UNS C64200 (Al-Si-Bronze) and UNS C63200 (Ni-Al-Bronze). *Journal of failure analysis and prevention*, 13, 8-19.

- Li, Zhiyuan; Yan, Hua; Zhang, Peilei; Guo, Jialong; Yu, Zhishui; Ringsberg, Jonas W. (2021): Improving surface resistance to wear and corrosion of nickel-aluminum bronze by laser-clad TaC/Co-based alloy composite coatings. In *Surface and Coatings Technology* 405, p. 126592. DOI: 10.1016/j.surfcoat.2020.126592.
- Mousavi, Seyed Elias; Naghshehkesh, Nastaran; Amirnejad, Mohabbat; Shammakhi, Hossein; Sonboli, Ali (2021): Wear and Corrosion Properties of Stellite-6 Coating Fabricated by HVOF on Nickel–Aluminium Bronze Substrate. In *Met. Mater. Int.* 27 (9), pp. 3269–3281. DOI: 10.1007/s12540-020-00697-7
- Pei, Y.T., Ocelik, V., Hosson, J.T.M. de, (2002). SiCp/Ti6Al4V functionally graded materials produced by laser melt injection. *Acta Materialia* 50, 2035–2051.